

# Effect of Deprotonation of a Benzimidazolyl Ligand on the Redox Potential and the Structures of Mononuclear Ruthenium(II) Complexes

Hongfei Sun,<sup>[a]</sup> Mei Wang,<sup>\*[a]</sup> Kun Jin,<sup>[a]</sup> Chengbing Ma,<sup>[b]</sup> Rong Zhang,<sup>[a]</sup> and Licheng Sun<sup>\*[a,c]</sup>

**Keywords:** Benzimidazolyl ligand / Redox switch / Reversible protonation and deprotonation / Ru<sup>II</sup> complex

A monoruthenium(II) complex of the benzimidazolyl ligand and its deprotonated counterpart were prepared and structurally characterized. The reversible protonation/deprotonation process of the ancillary ligand switches the redox po-

tential of the ruthenium(II) core from 0.69 to 0.26 V vs. Ag/AgNO<sub>3</sub>.  
(© Wiley-VCH Verlag GmbH & Co. KGaA, 69451 Weinheim, Germany, 2007)

## Introduction

Reversible protonation/deprotonation of an ancillary ligand at a site remote from the metal–ligand bond is a simple reaction but a crucial step in some complicated biological processes. Many metal-containing proteins and enzymes, such as photosystem II,<sup>[1,2]</sup> cytochrome *c* oxidase<sup>[3,4]</sup> and non-heme iron enzymes,<sup>[5]</sup> play their function involving proton-coupled electron transfer (PCET) reactions. To understand the relationship between electron transfer and proton motion, the PCET reactions and the modulation of the redox potential of biomimetic model complexes by deprotonation of the ligand have been intensively studied.<sup>[6–9]</sup> In most cases, imidazole, benzimidazole and biimidazole ligands were used as proton carriers because the metal centres of many metalloenzymes are coordinated by imidazole units from histidine residues.<sup>[10–12]</sup> The effect of the distal deprotonation of the ligands bearing imidazole and benzimidazole units on the physical and chemical properties of mono- and dinuclear ruthenium and osmium complexes has been reported.<sup>[13–19]</sup> In addition to the imidazole-containing ligands, mono- and dinuclear ruthenium complexes with ligands bearing triazole and pyrazole units were also extensively studied for their interesting electrochemical and photophysical properties.<sup>[20–24]</sup> In this communication, we

describe the preparation of the mononuclear ruthenium(II) complex [Ru(bbpaH)(bpy)](PF<sub>6</sub>)<sub>2</sub> [bbpaH = (2-benzimidazolylmethyl)bis(2-pyridylmethyl)amine, bpy = bipyridine], the influence of reversible protonation/deprotonation of the coordinated benzimidazolyl ligand on the redox potential of the ruthenium(II) complex, and the molecular structures of [Ru(bbpaH)(bpy)](PF<sub>6</sub>)<sub>2</sub> (**1**) and its deprotonated species [Ru(bbpa)(bpy)](PF<sub>6</sub>) (**2**). This proton-coupled redox process might be relevant to some metalloenzymes active sites, such as the oxygen evolving complex (OEC) in photosystem II.

## Results and Discussion

The starting complex [Ru(bbpaH)(dmsO)Cl](PF<sub>6</sub>)<sub>2</sub> was prepared by the reaction of Ru(dmsO)<sub>4</sub>Cl<sub>2</sub><sup>[25]</sup> and the bbpaH ligand<sup>[26]</sup> according to the literature procedure for the preparation of the analogous complex [Ru(tpa)(dmsO)Cl](PF<sub>6</sub>) [tpa = tris(2-pyridylmethyl)amine].<sup>[27]</sup> The subsequent reaction of [Ru(bbpaH)(dmsO)Cl](PF<sub>6</sub>) with bipyridyl as ligand at room temperature afforded the target complex [Ru(bbpaH)(bpy)](PF<sub>6</sub>)<sub>2</sub> in moderate yield. The deprotonated species [Ru(bbpa)(bpy)](PF<sub>6</sub>) was readily obtained by dissolving [Ru(bbpaH)(bpy)](PF<sub>6</sub>)<sub>2</sub> in an acetone/water (1:1, v/v) mixture with pH = 11. Both complexes are stable in polar aprotic solvent such as acetone and acetonitrile.

The molecular structures of [Ru(bbpaH)(bpy)]<sup>2+</sup> and its deprotonated species [Ru(bbpa)(bpy)]<sup>+</sup> were determined at –80 °C by X-ray diffraction analyses. To the best of our knowledge, these are the first crystallographically characterized protonation/deprotonation pair of ruthenium complexes containing an imidazolyl ligand. The overall structures of both complexes are very similar (Figure 1), with distorted octahedral coordination geometry around their ruthenium centres. In both complexes, two N<sub>py</sub> atoms, one from the bbpaH or bbpa ligand and another from the bpy

[a] State Key Laboratory of Fine Chemicals, DUT-KTH Joint Education and Research Centre on Molecular Devices, Dalian University of Technology, Zhongshan Road 158-46, Dalian 116012, P. R. China  
Fax: +86-411-83702185  
E-Mail: symbuono@dlut.edu.cn

[b] State Key Laboratory of Structural Chemistry, Fujian Institute of Research on the Structure of Matter, Fuzhou 350002, P. R. China

[c] Organic Chemistry, Royal KTH Chemical Science and Engineering, 10044, Stockholm, Sweden

Supporting information for this article is available on the WWW under <http://www.eurjic.org> or from the author.

ligand, an  $N_{\text{benz}}$  and an  $N_{\text{amine}}$  atom are located in a tetragonal plane. The remaining two  $N_{\text{py}}$  atoms occupy the vertices of the octahedron. The ruthenium atom in each complex lies slightly out of the tetragonal plane towards the pyridyl group of the bpy ligand, 0.0351 Å for  $[\text{Ru}(\text{bbpaH})(\text{bpy})]^{2+}$  and 0.0314 Å for  $[\text{Ru}(\text{bbpa})(\text{bpy})]^+$ . The Ru(1)–N(1) bond length increases significantly in the deprotonated species, 2.058(6) Å for  $[\text{Ru}(\text{bbpaH})(\text{bpy})]^{2+}$  and 2.100(3) Å for  $[\text{Ru}(\text{bbpa})(\text{bpy})]^+$ . In parallel, the Ru(1)–N(5) bond [2.064(3) Å] of  $[\text{Ru}(\text{bbpa})(\text{bpy})]^+$ , *trans* to the Ru(1)–N(1) bond, considerably shortens as compared to that [2.088(6) Å] of  $[\text{Ru}(\text{bbpaH})(\text{bpy})]^{2+}$ . The bond angles increase by ca. 18° for N(1)–Ru(1)–N(4) and 5° for N(1)–Ru(1)–N(6), while the N(1)–Ru(1)–N(7), N(1)–Ru(1)–N(3) and N(1)–Ru(1)–N(5) angles decrease by ca. 8, 4 and 1°, respectively, in the deprotonated complex. The other corresponding Ru–N bond lengths and N–Ru–N angles in the coordination sphere of two ruthenium complexes are quite similar. To the best of our knowledge there are only two examples of crystallographically characterized iron and cobalt complexes containing deprotonated imidazolylate and benzimidazolylate ligands.<sup>[8,9]</sup> The deprotonation of 2,6-bis(2-imidazolyl)pyridine as ligand in the iron complex leads to the oxidation of the iron(II) centre from  $\text{Fe}^{\text{II}}$  to  $\text{Fe}^{\text{III}}$ ,<sup>[9]</sup> while the formal oxidation state of the cobalt(II) centre in the cobalt complex of the tris(2-benzimidazolylmethyl)amine ligand does not change before and after deprotonation. During deprotonation, the ruthenium complex  $[\text{Ru}(\text{bbpaH})(\text{bpy})]^{2+}$  behaves like the cobalt complex. Compared with the molecular structures of the reported cobalt complexes, there are two noteworthy points in the molecular structure of the deprotonated ruthenium complex. First, the lengthening of 0.042 Å for the Ru– $N_{\text{benzimidazolylate}}$  bond is contrary to the shortening of 0.026 Å for the Co– $N_{\text{benzimidazolylate}}$  bond.<sup>[8]</sup> Second, the length of the Ru– $N_{\text{py}}$  bond *trans* to the Ru– $N_{\text{benzimidazolylate}}$  bond decreases by 0.024 Å in the deprotonated ruthenium complex, while one of the Co– $N_{\text{benz}}$  bonds neighbouring

the Co– $N_{\text{benzimidazolylate}}$  bond increases by 0.053 Å. These apparent contrasts in the changes of the M–N bond lengths after deprotonation of the prepared ruthenium complex and the reported cobalt complex are assumed to result from the strong coordination ability of the pyridyl group and from different coordination geometries of the ruthenium and cobalt complexes. In spite of the differences in the aforementioned two aspects, the lengthening (0.005 Å) of the average distance of the Ru–N bonds in the tetragonal plane of  $[\text{Ru}(\text{bbpa})(\text{bpy})]^+$ , as compared to that of the parent ruthenium complex, is consistent with the 0.009 Å increase in that of the Co–N bonds in the trigonal plane for the deprotonated cobalt complex.

The reversible protonation/deprotonation process was monitored by ESI mass spectrometry and  $^1\text{H}$  NMR spectroscopy. The ESI mass spectra of  $[\text{Ru}(\text{bbpaH})(\text{bpy})]^{2+}$  and the deprotonated complex  $[\text{Ru}(\text{bbpa})(\text{bpy})]^+$  show signature peaks at  $m/z = 293.6$  and 586.1, respectively. Figure 2 shows the curves of relative intensities of the peaks for  $[\text{Ru}(\text{bbpaH})(\text{bpy})]^{2+}$  and  $[\text{Ru}(\text{bbpa})(\text{bpy})]^+$  vs. the equiv. of  $\text{NEt}_3$  in the acetone solution of complex **1**. As shown in Figure 2, the peak at  $m/z = 586.1$  for  $[\text{Ru}(\text{bbpa})(\text{bpy})]^+$  is enhanced gradually with the addition of  $\text{NEt}_3$ , and the peak at  $m/z = 293.6$  for  $[\text{Ru}(\text{bbpaH})(\text{bpy})]^{2+}$  eventually disappears in the presence of 2 equiv. of  $\text{NEt}_3$ . No peak for dinuclear or larger cluster is found in mass spectra in the presence of  $\text{NEt}_3$ .

The  $^1\text{H}$  NMR spectra of a selected region for  $[\text{Ru}(\text{bbpaH})(\text{bpy})](\text{PF}_6)_2$  and the deprotonated complex  $[\text{Ru}(\text{bbpa})(\text{bpy})](\text{PF}_6)$  in  $[\text{D}_6]\text{acetone}$  are shown in Figure 3. The six methylene protons are all inequivalent with respect to their chemical environment, and each  $\text{CH}_2$  group displays an AB quartet (Figure 3a). Compared with the  $^1\text{H}$  NMR spectra of the reported complex coordinated by the ligands bearing 2-pyridylmethyl moieties,<sup>[28]</sup> the quartet centered at  $\delta = 5.08$  is attributed to the  $\text{CH}_2$  group attached to the benzimidazolyl unit, and the other two quartets to the  $\text{CH}_2$  groups of the pyridylmethyl units. Upon addition

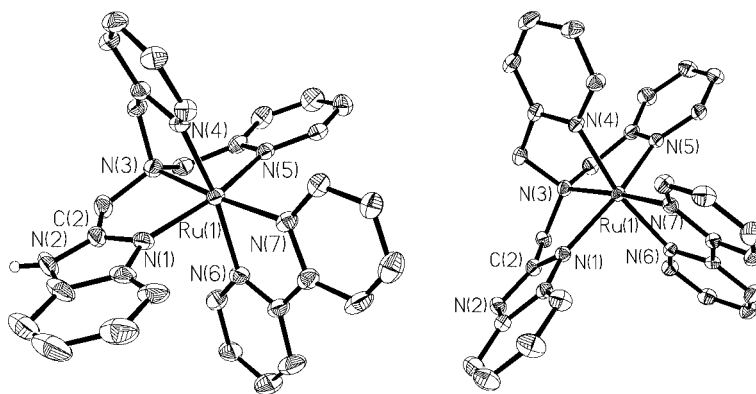


Figure 1. Thermal ellipsoid diagram of  $[\text{Ru}(\text{bpbaH})(\text{bpy})]^{2+}$  (left) and  $[\text{Ru}(\text{bpba})(\text{bpy})]^+$  (right). The ellipsoids are drawn at the 30% probability level, and only the benzimidazolyl hydrogen atom is shown. Selected bond lengths [Å] and angles [°] for  $[\text{Ru}(\text{bpbaH})(\text{bpy})]^{2+}$  and  $[\text{Ru}(\text{bpba})(\text{bpy})]^+$  [in brackets]: Ru(1)–N(1), 2.058(6) [2.100(3)]; Ru(1)–N(3), 2.119(6) [2.113(3)]; Ru(1)–N(4), 2.088(6) [2.100(3)]; Ru(1)–N(5), 2.088(6) [2.064(3)]; Ru(1)–N(6), 2.090(6) [2.090(3)]; Ru(1)–N(7), 2.072(6) [2.076(3)]; C(2)–N(1), 1.343(9) [1.366(4)]; C(2)–N(2), 1.354(10) [1.334(5)]; N(1)–Ru(1)–N(3), 82.2(2) [78.69(11)]; N(1)–Ru(1)–N(4), 82.3(2) [100.53(11)]; N(1)–Ru(1)–N(5), 161.4(2) [160.55(11)]; N(1)–Ru(1)–N(6), 86.6(2) [91.50(10)]; N(1)–Ru(1)–N(7), 103.1(2) [95.39(10)].

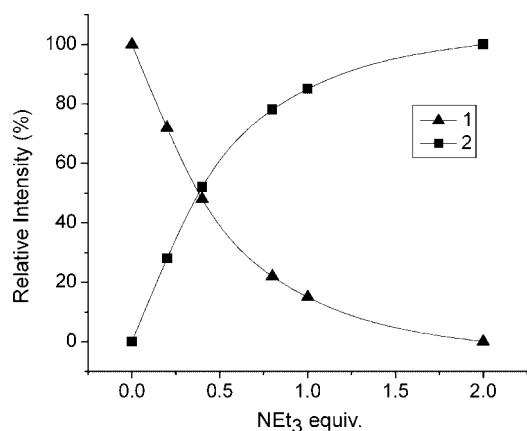


Figure 2. Plot of relative intensities of the peaks for  $[\text{Ru}(\text{bbpaH})(\text{bpy})]^{2+}$  (triangle) and  $[\text{Ru}(\text{bbpa})(\text{bpy})]^+$  (square) vs. the equiv. of  $\text{NEt}_3$  (0, 0.2, 0.4, 0.6, 1.0, 2.0 equiv.) in an acetone solution of complex **1** ( $5 \times 10^{-4}$  M) monitored by ESI-MS.

of 2 equiv. of  $\text{NEt}_3$ , the signals for  $[\text{Ru}(\text{bbpaH})(\text{bpy})](\text{PF}_6)_2$  completely disappear, and only the signals for  $[\text{Ru}(\text{bbpa})(\text{bpy})](\text{PF}_6)$  are detected (Figure 3b), which suggests that no other reaction or decomposition occurs during the deprotonation process. Significant upfield shifts are observed in Figure 3b for the corresponding signals of three  $\text{CH}_2$  groups of the deprotonated complex, which are expected for the monoanionic  $\text{bbpa}^-$  ligand. The quartet at  $\delta = 5.08$  in the  $^1\text{H}$  NMR spectrum of  $[\text{Ru}(\text{bbpaH})(\text{bpy})](\text{PF}_6)_2$  changes to a singlet at  $\delta = 4.78$  upon deprotonation, indicating that the two protons on the  $\text{CH}_2$  group of the benzimidazolymethyl arm gain better symmetry in the deprotonated complex. The signals for the benzene ring of the deprotonated benzimidazolymethyl ligand also apparently shift upfield. Sequential addition of 1 equiv. of  $\text{HClO}_4$  recovers the original  $^1\text{H}$  NMR spectrum of  $[\text{Ru}(\text{bbpaH})(\text{bpy})](\text{PF}_6)_2$  as depicted in Figure 3a. This clearly indicates the complete reversibility of deprotonation and protonation.

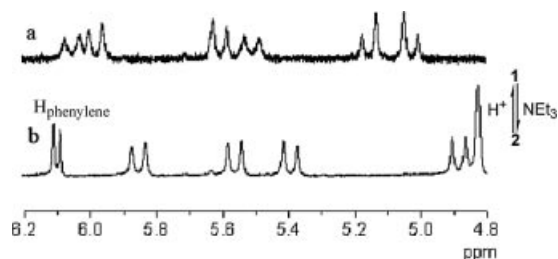


Figure 3.  $^1\text{H}$  NMR spectra of a selected region: (a)  $[\text{Ru}(\text{bbpaH})(\text{bpy})](\text{PF}_6)_2$  (**1**) and (b)  $[\text{Ru}(\text{bbpa})(\text{bpy})](\text{PF}_6)$  (**2**) in  $[\text{D}_6]\text{acetone}$ .

The influence of deprotonation of the coordinated  $\text{bbpaH}$  ligand on the redox potential of the ruthenium centre was explored by cyclic voltammograms. The reversible  $\text{Ru}^{\text{II}}/\text{Ru}^{\text{III}}$  oxidation wave of  $[\text{Ru}(\text{bbpaH})(\text{bpy})](\text{PF}_6)_2$  appears at 0.69 V ( $E_{1/2}$ ) vs.  $\text{Ag}/\text{AgNO}_3$  in  $\text{CH}_3\text{CN}$  and the deprotonated ruthenium complex  $[\text{Ru}(\text{bbpa})(\text{bpy})](\text{PF}_6)$  displays the reversible oxidation wave at 0.26 V (Figures S1

and S2, see Supporting Information). It shows that the deprotonation of the coordinated  $\text{bbpaH}$  ligand can shift the redox potential of the ruthenium centre by 430 mV, which is larger than the shift (ca. 300–350 mV per proton) of the redox potentials reported for ruthenium, osmium and iron complexes with the ligands bearing multi-imidazolyl and -benzimidazolyl units,<sup>[9,14–16]</sup> but similar to the shift (350–420 mV) of the  $\text{Ru}^{\text{II}}/\text{Ru}^{\text{III}}$  oxidation potentials reported for monoruthenium complexes with two bpy ligands and one triazole- or pyrazole-containing ligand.<sup>[21,23,29,30]</sup>

## Conclusions

We have prepared a pair of novel monoruthenium(II) complexes (**1** and **2**) with  $\text{bbpaH}$  or  $\text{bbpa}$  and bipyridine as ligands. The structures of (benzimidazole)ruthenium complexes **1** and **2** were crystallographically characterized. The NH group of the  $\text{bbpaH}$  ligand readily undergoes a reversible protonation/deprotonation process, which is proven by spectroscopic and electrochemical evidence. The reversible protonation/deprotonation regulates the oxidation potential of the  $\text{Ru}^{\text{II}}/\text{Ru}^{\text{III}}$  redox couple around 430 mV without changing the framework of the ruthenium complex.

## Experimental Section

**General Procedures:** All reactions and operations related to organometallic complexes were carried out under dry, oxygen-free dinitrogen with standard Schlenk techniques. Solvents were distilled prior to use with routine drying agents. Tetra-*n*-butylammonium hexafluorophosphate (TBAH) and bipyridine were used as received. Ligand (2-benzimidazolymethyl)bis(2-pyridylmethyl)amine ( $\text{bbpaH}$ ) and  $[\text{Ru}(\text{bbpa})(\text{dmsO})\text{Cl}](\text{PF}_6)$  were synthesized according to literature procedures for preparation of similar compounds.<sup>[25–27]</sup>  $^1\text{H}$  NMR spectra were collected with a Varian INOVA 400 NMR spectrometer. Elemental analyses were performed with a Thermoquest-Flash EA 1112 elemental analyzer. Mass spectra were recorded with an HP 1100 MSD instrument.

**Complex  $[\text{Ru}(\text{bbpaH})(\text{bpy})](\text{PF}_6)_2$  (**1**):** Complex **1** was synthesized according to a literature procedure for the preparation of the analogous complex  $[\text{Ru}(\text{TPA})(\text{bpy})](\text{PF}_6)_2$ .<sup>[27]</sup> The subsequent recrystallization of the crude product from acetone/diethyl ether afforded red crystals. Yield: 94 mg (37%).  $^1\text{H}$  NMR ( $\text{CDCl}_3$ , 400 MHz):  $\delta = 10.21$  (d, 1 H,  $J = 5.6$  Hz, Py of  $\text{bbpaH}$ ), 9.47 (d,  $J = 6.0$  Hz, 1 H, Py of bpy), 9.44 (d,  $J = 6.0$  Hz, 1 H, Py of bpy), 8.80 (d,  $J = 8.2$  Hz, 1 H, Py of  $\text{bbpaH}$ ), 8.59 (d,  $J = 8.0$  Hz, 1 H, Py of  $\text{bbpaH}$ ), 8.42 (t,  $J = 8.2$ , 7.4 Hz, 1 H, Py of  $\text{bbpaH}$ ), 8.21 (t,  $J = 5.6$ , 7.4 Hz, 1 H, Py of  $\text{bbpaH}$ ), 7.96 (t,  $J = 8.0$ , 6.4 Hz, 1 H, Py of  $\text{bbpaH}$ ), 7.94 (t,  $J = 5.8$ , 7.2 Hz, 1 H, Py of bpy), 7.78 (d,  $J = 7.8$  Hz, 1 H, Py of  $\text{bbpaH}$ ), 7.77 (d,  $J = 5.8$  Hz, 1 H, Py of bpy), 7.73 (t,  $J = 6.4$ , 6.4 Hz, 1 H, Py of bpy), 7.59 (d,  $J = 6.4$  Hz, 1 H, Py of bpy), 7.53 (t,  $J = 7.8$ , 6.4 Hz, 1 H, Py of  $\text{bbpaH}$ ), 7.53 (d,  $J = 6$  Hz, 1 H, Py of bpy), 7.43 (d,  $J = 8.4$  Hz, 1 H, Ph of  $\text{bbpaH}$ ), 7.33 (t,  $J = 6.0$ , 6.4 Hz, 1 H, Py of bpy), 7.15 (t,  $J = 8.4$ , 7.2 Hz, 1 H, Ph of  $\text{bbpaH}$ ), 7.00 (t,  $J = 7.2$ , 8.0 Hz, 1 H, Ph of  $\text{bbpaH}$ ), 6.50 (d,  $J = 8.0$  Hz, 1 H, Ph of  $\text{bbpaH}$ ), 6.02 (d,  $J = 18.4$  Hz, 1 H, CH of  $\text{bbpaH}$ ), 5.96 (d,  $J = 18.4$  Hz, 1 H, CH of  $\text{bbpaH}$ ), 5.58 (d,  $J = 16.8$  Hz, 1 H, CH of  $\text{bbpaH}$ ), 5.48 (d,  $J = 17.6$  Hz, 1 H, CH of  $\text{bbpaH}$ ), 5.13 (d,  $J = 16.8$  Hz, 1 H, CH of  $\text{bbpaH}$ ), 5.01 (d,  $J = 17.6$  Hz, 1 H, CH of  $\text{bbpaH}$ ) ppm. ESI-MS:  $m/z = 293.5$   $[\text{Ru}(\text{bbpaH})(\text{bpy})]^{2+}$ .

$C_{31.5}H_{30}F_{12}N_7O_{0.5}P_2Ru$  (905.62): calcd. C 41.72, H 2.82, N 10.83; found C 41.75, H 2.73, N 10.83.

**Complex [Ru(bbpa)(bpy)](PF<sub>6</sub>) (2):** Complex 1 (50 mg, 0.057 mmol) was dissolved in an NaOH-containing acetone/water (1:1, v/v) mixture with pH = 11. A majority of the acetone was removed in a rotary evaporator and the product precipitated as the fully deprotonated species [Ru(bbpa)(bpy)](PF<sub>6</sub>). The solid was dissolved in hot CHCl<sub>3</sub>. After cooling, dark-red crystals were obtained. Yield: 13 mg (31%). <sup>1</sup>H NMR (CDCl<sub>3</sub>, 400 MHz): δ = 10.15 (d, 1 H, *J* = 6.0 Hz, Py of bbpa), 9.37 (d, *J* = 5.6 Hz, 1 H, Py of bbpa), 9.32 (d, *J* = 6.0 Hz, 1 H, Py of bpy), 8.71 (d, *J* = 8.0 Hz, 1 H, Py of bbpa), 8.49 (d, *J* = 8.0 Hz, 1 H, Py of bbpa), 8.30 (t, *J* = 6.8, 8.0 Hz, 1 H, Py of bbpa), 8.07 (t, *J* = 6.0, 6.8 Hz, 1 H, Py of bbpa), 7.98 (d, *J* = 5.6 Hz, 1 H, Py of bpy), 7.81 (t, *J* = 7.2, 8.0 Hz, 1 H, Py of bbpa), 7.68 (t, *J* = 7.2, 7.6 Hz, 1 H, Py of bpy), 7.58 (t, *J* = 7.6, 6.8 Hz, 1 H, Py of bpy), 7.57 (d, *J* = 7.6 Hz, 1 H, Py of bpy), 7.39 (t, *J* = 5.6, 7.2 Hz, 1 H, Py of bbpa), 7.38 (d, *J* = 6.8 Hz, 1 H, Py of bpy), 7.20 (d, *J* = 8.4 Hz, 1 H, Ph of bbpa), 7.17 (t, *J* = 6.0, 7.2 Hz, 1 H, Py of bpy), 7.14 (t, *J* = 5.6, 7.6 Hz, 1 H, Py of bpy), 6.64 (t, *J* = 8.4, 7.6 Hz, 1 H, Ph of bbpa), 6.51 (t, *J* = 7.6, 7.6 Hz, 1 H, Ph of bbpa), 6.10 (d, *J* = 7.6 Hz, 1 H, Ph of bbpa), 5.85 (d, *J* = 16.8 Hz, 1 H, CH of bbpa), 5.56 (d, *J* = 16.4 Hz, 1 H, CH of bbpa), 5.39 (d, *J* = 16.8 Hz, 1 H, CH of bbpa), 4.89 (d, *J* = 16.4 Hz, 1 H, CH of bbpa), 4.83 (s, 2 H, CH<sub>2</sub> of bbpa) ppm. ESI-MS: *m/z* = 586.1 [Ru(bbpa)(bpy)]<sup>+</sup>. C<sub>31</sub>H<sub>27</sub>Cl<sub>3</sub>F<sub>6</sub>N<sub>7</sub>PRu (849.99): calcd. C 43.80, H 3.20, N 11.54; found C 44.79, H 3.27, N 11.68.

**X-ray Structure Determination:** The single-crystal X-ray diffraction data were collected with a Siemens SMART CCD diffractometer, with graphite-monochromated Mo-K<sub>α</sub> radiation ( $\lambda = 0.071073 \text{ \AA}$ ) at 153 K using the  $\omega$ -2 $\theta$  scan mode. Data processing was accomplished with the SAINT processing program.<sup>[31]</sup> Intensity data were corrected for absorption by the SADABS program.<sup>[32]</sup> All structures were solved by direct methods and refined on *F*<sup>2</sup> by full-matrix least-squares methods using the SHELXTL 97 program package.<sup>[33]</sup> All non-hydrogen atoms were refined anisotropically. Hydrogen atoms were located by geometrical calculation. Crystal data for [Ru(bbpaH)(bpy)](PF<sub>6</sub>)<sub>2</sub> (1): C<sub>30.50</sub>H<sub>29</sub>F<sub>12</sub>N<sub>7</sub>O<sub>0.50</sub>P<sub>2</sub>Ru, *M* = 892.62, monoclinic, space group *P*2(1)/*n*, *a* = 12.4535(14), *b* = 19.742(2), *c* = 13.6163(15) Å,  $\beta = 91.270^\circ$ , *V* = 3346.8(6) Å<sup>3</sup>, *Z* = 4,  $\rho_{\text{calcd.}} = 1.772 \text{ g cm}^{-3}$ ,  $\mu = 0.67 \text{ mm}^{-1}$ , *T* = 153(2) K, 6565 reflections measured, 4243 unique, *R*<sub>int</sub> = 0.0650, *R*<sub>1</sub> = 0.0787 and *wR*<sub>2</sub> = 0.1138 (all data), GOF = 1.017. CCDC-641251. Crystal data for [Ru(bbpa)(bpy)](PF<sub>6</sub>) (2): C<sub>32</sub>H<sub>29</sub>Cl<sub>3</sub>F<sub>6</sub>N<sub>7</sub>PRu, *M* = 934.91, triclinic, space group *P*1, *a* = 10.6539(7), *b* = 13.1807(9), *c* = 13.9109(9) Å,  $\alpha = 75.291^\circ$ ,  $\beta = 75.424^\circ$ ,  $\gamma = 84.229^\circ$ , *V* = 1827.2(2) Å<sup>3</sup>, *Z* = 2,  $\rho_{\text{calcd.}} = 1.699 \text{ g cm}^{-3}$ ,  $\mu = 0.91 \text{ mm}^{-1}$ , *T* = 153(2) K, 7046 reflections measured, 5985 unique, *R*<sub>int</sub> = 0.0192, *R*<sub>1</sub> = 0.0531, *wR*<sub>2</sub> = 0.1123 (all data), GOF = 1.028. CCDC-641252. These data can be obtained free of charge from The Cambridge Crystallographic Data Centre via [www.ccdc.cam.ac.uk/data\\_request/cif](http://www.ccdc.cam.ac.uk/data_request/cif).

**Supporting Information** (see footnote on the first page of this article): Figures S1 and S2 give cyclic voltammograms of [Ru(bbpaH)(bpy)](PF<sub>6</sub>)<sub>2</sub> (1) and [Ru(bbpa)(bpy)](PF<sub>6</sub>) (2).

## Acknowledgments

We are grateful to the Chinese National Natural Science Foundation (Grant nos. 20471013 and 20633020), the Swedish Energy Agency, the Swedish Research Council and K & A Wallenberg Foundation for financial support of this work.

- [1] M. Y. Okamura, G. Feher, *Annu. Rev. Biochem.* **1992**, *61*, 861–896.
- [2] G. T. Babcock, B. A. Barry, R. J. Debus, C. W. Hoganson, M. Atamian, L. McIntosh, I. Sithole, C. F. Yocum, *Biochemistry* **1989**, *28*, 9557–9565.
- [3] B. Maison-Peteri, B. G. Malmstrom, *Biochemistry* **1989**, *28*, 3156–3160.
- [4] J. E. Morgan, M. Wikstrom, *Biochemistry* **1991**, *30*, 948–958.
- [5] A. L. Feig, S. J. Lippard, *Chem. Rev.* **1994**, *94*, 759–805.
- [6] T. Claudia, C. K. Chang, G. E. Leroi, R. I. Cukier, D. G. Nocera, *J. Am. Chem. Soc.* **1992**, *114*, 4013–4015.
- [7] J. P. Kirby, J. A. Roberts, D. G. Nocera, *J. Am. Chem. Soc.* **1997**, *119*, 9230–9236.
- [8] B. S. Hammes, M. T. Kieber-Emmons, R. Sommer, A. L. Rheingold, *Inorg. Chem.* **2002**, *41*, 1351–1353.
- [9] R. F. Carina, L. Verzegnassi, A. F. Williams, *Chem. Commun.* **1998**, 2681–2682.
- [10] S. Han, L. D. Eltis, K. N. Timmis, S. W. Muchmore, J. T. Bolin, *Science* **1995**, *270*, 976–980.
- [11] J. C. Boyington, B. J. Gaffney, M. Arnez, *Science* **1993**, *260*, 1482–1486.
- [12] P. L. Roach, I. J. Clifton, V. Fülöp, K. Harlos, G. J. Barton, J. Hajdu, I. Andersson, C. J. Schofield, J. E. Baldwin, *Nature* **1995**, *375*, 700–704.
- [13] A. M. Bond, M. Haga, *Inorg. Chem.* **1986**, *25*, 4507–4514.
- [14] M. Haga, T. Ano, K. Kano, S. Yamabe, *Inorg. Chem.* **1991**, *30*, 3843–3849.
- [15] M. Haga, T. Ano, K. Kano, K. Nozaki, T. Ohno, *J. Chem. Soc. Dalton Trans.* **1994**, 263–272.
- [16] M. Haga, M. M. Ali, A. S. Koseki, K. Fujimoto, A. Yoshimura, K. Nozaki, T. Ohno, K. Nakajima, D. J. Stufkens, *Inorg. Chem.* **1996**, *35*, 3335–3347.
- [17] S. Baitalik, U. Flörke, K. Nag, *Inorg. Chem.* **1999**, *38*, 3296–3308.
- [18] S. Baitalik, P. Bag, K. Nag, *Polyhedron* **2002**, *21*, 2481–2488.
- [19] S. Baitalik, B. Dutta, K. Nag, *Polyhedron* **2004**, *23*, 913–919.
- [20] R. Hage, J. G. Haasnoot, J. Reedijk, R. Wang, J. G. Vos, *Inorg. Chem.* **1991**, *30*, 3263–3269.
- [21] H. E. B. Lempers, J. G. Haasnoot, J. Reedijk, R. Hage, F. M. Weldon, J. G. Vos, *Inorg. Chim. Acta* **1994**, *225*, 67–74.
- [22] C. D. Pietro, S. Serroni, S. Campagna, M. T. Gandolfi, R. Ballardini, S. Fanni, W. R. Browne, J. G. Vos, *Inorg. Chem.* **2002**, *41*, 2871–2878.
- [23] C. Sens, M. Rodríguez, I. Romero, A. Llobet, *Inorg. Chem.* **2003**, *42*, 2040–2048.
- [24] C. Sens, M. Rodríguez, I. Romero, A. Llobet, *Inorg. Chem.* **2003**, *42*, 8385–8394.
- [25] I. P. Evans, A. Spencer, G. Wilkinson, *J. Chem. Soc. Dalton Trans.* **1973**, 204–209.
- [26] M. Psacaly, M. Duda, F. Schweppe, K. Zurlinden, F. K. Müller, B. Krebs, *J. Chem. Soc. Dalton Trans.* **2001**, 828–837.
- [27] J. Bjernemose, A. Hazell, C. J. McKenzie, M. F. Mahon, L. P. Nielsen, P. R. Raitby, O. Simonsen, H. Toftlund, J. A. Wolny, *Polyhedron* **2003**, *22*, 875–885.
- [28] T. Kojima, T. Sakamoto, Y. Matsuda, *Inorg. Chem.* **2004**, *43*, 2243–2245.
- [29] B. D. J. R. Fennema, R. Hage, J. G. Haasnoot, J. Reedijk, *Inorg. Chim. Acta* **1990**, *171*, 223–228.
- [30] H. A. Nieuwenhuis, J. G. Haasnoot, R. Hage, J. Reedijk, T. L. Snoeck, D. J. Stufkens, J. G. Vos, *Inorg. Chem.* **1991**, *30*, 48–54.
- [31] Software packages *SMART* and *SAINTE*, Siemens Energy & Automation Inc., Madison, Wisconsin, **1996**.
- [32] G. M. Sheldrick, *SADABS, Absorption Correction Program*, University of Göttingen, Germany, **1996**.
- [33] G. M. Sheldrick, *SHELXTL 97, Program for the Refinement of Crystal Structure*, University of Göttingen, Germany, **1997**.

Received: May 25, 2007

Published Online: August 7, 2007